Polarized operation of Yb^{3+}:$YAl_3(BO_3)_4$ CW and mode-locked lasers

Yanrong Song (宋晏蓉)[1] and Qingyue Wang (王清月)[2]

[1] *School of Applied Science, Beijing University of Technology, Beijing 100022*

[2] *School of Precision Instrument and Optoelectronics Engineering, University of Tianjin, Tianjin 300072*

Received September 23, 2004

A diode-pumped Yb^{3+}:$YAl_3(BO_3)_3$ (Yb:YAB) laser system was demonstrated with continuous wave (CW) and pulsed output. The polarized CW outputs and femtosecond mode-locked lasers with semiconductor saturable-absorber mirrors (SESAM) at the fundamental wavelength were measured. For the CW output, polarization ratios were 88.1% (for e-ray) and 87.2% (for o-ray). For the mode-locked system, polarization ratio reached 38.5%, and the repetition frequency was 117.6 MHz.

OCIS codes: 140.0140, 140.4050, 140.3480, 140.3580, 160.4760.

The absorption bands of ytterbium (Yb^{3+})-doped crystals around 0.97 μm are well-suited for pumping by efficient InGaAs diode lasers which have been developed over the past decade. The small quantum defect for Yb results in highly efficient laser operation, which is not degraded by concentration quenching or excited-state absorption. High doping concentrations enable shorter crystal lengths to be employed, leading to compact diode-pumped systems. Compared with Nd^{3+}-doped materials, Yb^{3+}-doped crystals exhibit very broadband fluorescence, which allows tunability and/or ultra-short pulse generation, and the low material dispersion allows a narrower pulse width under mode-locked operation[1−3]. Several Yb^{3+}-doped femtosecond mode-locked lasers have been demonstrated in recent years by the use of semiconductor saturable-absorber mirrors (SESAM) or Kerr lens mode-locking mechanisms[4−8].

Interestingly, some of these crystals have high nonlinear coefficients that give them the potential for self-frequency-doubling (SFD) properties. One advantage of SFD is that both the fundamental and the self-doubled output are emitted simultaneously (and possibly collinearly). The disadvantage makes the output unstable due to the doubling, since both mode-locking and SFD effects depend on the intracavity power intensity.

When they exist simultaneously, they will affect each other and introduce instability. We chose to investigate the operation of Yb^{3+}:$YAl_3(BO_3)_4$ (Yb:YAB) a highly efficient SFD crystal[9], with wide wavelength tunability. To achieve stable laser operation, we investigated the polarization characteristics of the crystal to obtain stable polarized fundamental laser operation. In this paper, we describe diode-pumped, continuous wave (CW), mode-locked, and polarized Yb:YAB laser systems, using the crystal's spectral and birefringence characteristics without employing any extra elements in the laser system.

Yb:YAB is a negative uniaxial crystal. When entering the crystal, the monochromatic light separates into two waves: the ordinary wave (o-ray) and the extraordinary wave (e-ray). Normally, the spectra of the o-ray and the e-ray are termed σ-polarized and π-polarized spectra, respectively. Our crystals were cut for type 1 phase-matched frequency doubling at 1064 nm. This requires operation of the fundamental as the o-ray, with the frequency-doubled output as the e-ray. Figures 1 and 2 show the polarized absorption spectra and emission spectra, respectively, for Yb:YAB (The Yb dopant concentration was approximately 5 at.-%). From these figures we can see that the absorption and emission spectra show similar polarization characteristics. For the case of the absorption spectra, the σ-polarized absorption is much stronger than the π-polarized absorption. The strongest absorption peak is at 975 nm where the absorption coefficient is 9.0 cm^{-1} while the same parameter for the π-polarized absorption is 1.1 cm^{-1} at 983 nm. In all the experiments, the pump diode laser (from Unique-mode, Germany) was fibre-coupled with a slight residual polarization (typically 10:1). We adjusted

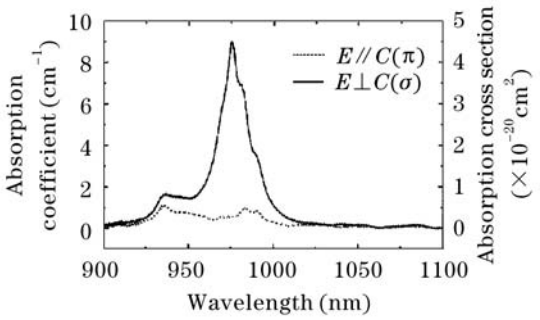

Fig. 1. The polarized absorption spectra. The solid line is for σ-polarization and the dashed line is for π-polarization.

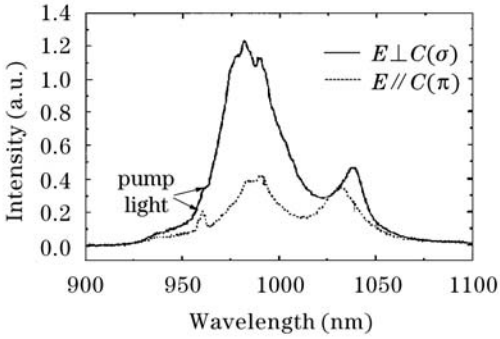

Fig. 2. Fluorescence spectra. The solid line is for σ-polarization and the dashed line is for π-polarization.

the fiber to match the crystal polarization for maximum pumping efficiency.

The polarized emission spectra have similar properties as above. For σ-polarization, there are two main broad emission bands in the ranges of 965—1002 nm and 1024—1045 nm, respectively. Although the band at 965—1002 nm is much stronger than that at 1024—1045 nm, there is significant absorption in this area. The same condition occurs for the π-polarized spectra. The amplitude difference between the σ-polarized and π-polarized emissions at long wavelengths is relatively small. Thus we selected an operating wavelength of 1038 nm for σ-polarization or 1030 nm for π-polarization operation. In order to obtain stable fundamental polarized laser output, we needed to suppress self-frequency doubling. Because the SFD effect for π-polarization is weaker than that for σ-polarization, we used the π-polarization as the output polarization. This is described in more detail below.

Normally a laser crystal is cut at Brewster's angle to produce a polarized laser. However, for diode-end-pumped lasers, it is necessary to use short-focal-length lenses to focus the pump light on the crystal, thus requiring that the distance between the input mirror and crystal be short (~1 mm). If the crystal is put at Brewster's angle, it is difficult to locate all the elements in the cavity. Thus to control the output polarization, we selected π-polarization as the output polarization using the ray walk-off caused by the crystal birefringence.

To set up the laser system, we first identified the crystal's ordinary and extraordinary light directions. A He-Ne laser was employed as a source. Yb:YAB crystal (cut for Type 1 phase-matched frequency doubling at 1064 nm) was placed between two focus lenses. Two spots were observed on the screen. The crystal was rotated perpendicularly to the He-Ne beam, and the unmoved spot corresponded to the o-ray, while the other spot circling around this spot was the e-ray. The crystal was aligned in the mount so that the line between the two spots was parallel to the optical table, and the two polarization directions were mutually orthogonal. One polarization was parallel to the table (e-ray) and the other polarization was perpendicular to the table (o-ray). Because of the walk-off effects of the ordinary and extraordinary lights, we selected the output polarization by twisting the cavity's end mirror.

Figure 3(a) and (b) show a short plano-concave

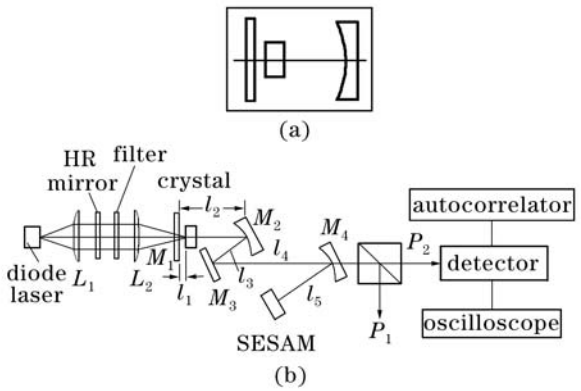

Fig. 3. System schemes of the CW laser (a) and the mode-locked laser (b).

cavity to obtain CW polarized output and a folded cavity to obtain mode locking output, respectively. The maximum output power from the 975-nm fibre-coupled pump laser was 2.8 W. The pump light was aligned and focused by two lenses onto the crystal. The dimensions of the Yb:YAB crystal were $3 \times 3 \times 3$ (mm), and it was antireflection coated for the fundamental. The input mirror was coated for high transmission at 976 nm and high reflection at 1020—1060 nm. For the CW laser, the curvature radius of the output mirror was 25 mm, and it was ~99 % reflectivity at the laser fundamental. The polarized output was tested with a Glan prism polarizer. When we adjusted the angle of the end mirror to get the e-ray laser, the polarized light parallel to the table (P_2) was 126 mW, while the output polarization (P_1) in the orthogonal direction (o-ray) was 8 mW. On the other hand, when we tried to make the o-ray polarization output larger, P_1 was 132 mW, while the e-ray polarization P_2 was 9 mW. We define that the polarization ratio is $|P_2 - P_1| / |P_2 + P_1|$. These data give polarization ratios of 88.1% and 87.2% respectively.

The same approach was used to investigate the SESAM mode-locked laser system. Because the doubling coefficient for the parallel polarization direction is weaker than that of the perpendicular polarization direction, we designed a parallel-polarized laser. We employed a SESAM as the end mirror and the saturable absorber to get mode-locked operation. The input mirror M_1 was coated for high transmission at 976 nm and high reflection at 1020—1060 nm. The curvature radii of mirrors M_2 and M_3 were 25 and 50 mm, respectively. There were two beam waists in the cavity, one at the input mirror M_1 so that the cavity mode spot size at the crystal matched the pump beam. Another was at the SESAM so as to increase the laser intensity to reach the saturation of the SESAM. The cavity length was about 78 cm. We obtained CW mode-locked laser operation with the SESAM, at a pulse repetition frequency of 117.6 MHz. The central wavelength was 1037 nm. Because a concave folding mirror (M_4) was used for the output mirror, two output beams were obtained, but only one was measured, with an output power of 14 mW. In order to test the polarization degree with this situation, we employed a Glan prism as same with the short cavity.

When the maximum output power at orthogonal direction (P_1) from the Glan prism was 4 mW, the output power at parallel direction output power (P_2) was 9 mW. If we still use the definition of the polarization ratio as above($|P_2 - P_1| / |P_2 + P_1|$), the polarization ratio reached 38.5%. Compared with the shorter CW laser, the mode-locked laser output power was much smaller. This was because that we employed a high reflecting concave mirror as the output mirror, but used a 99 % reflectivity mirror as the output mirror in the CW set up. We would expect higher output power from the mode-locked laser with a higher transmission output coupler. The polarization ratio in the mode-locked laser was not as high as for the CW laser. The main reason was that the intracavity intensity was higher when mode locking was operating, and the orthogonally-polarized laser mode could reach threshold. Figure 4 shows the spectrum of the pulsed laser (solid line) with a Gaussian fitting curve (dashed line). The spectrum is a near-perfect Gaussian and the

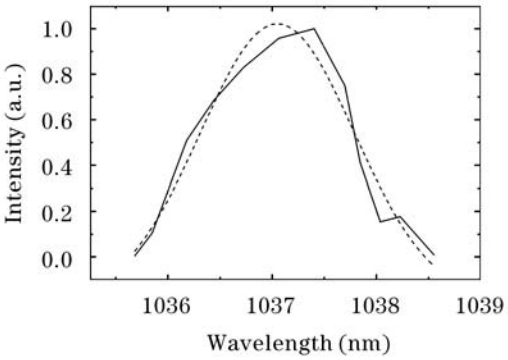

Fig. 4. The spectrum of the CW SESAM mode-locked laser (solid) and a Gaussian fitting curve (dash).

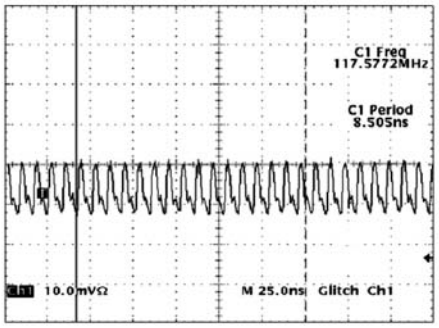

Fig. 5. The polarized output pulse train of the SESAM mode-locked laser.

pulse width is estimated from this as 640 fs. We did not compensate for the intracavity dispersion. After dispersion compensation, the pulse width would be expected to be shorter. Figure 5 shows the stability of the CW mode-locked pulse train.

In the paper, we have described two diode-pumped Yb:YAB laser systems. Using the birefringence of the crystal, we controlled the polarization of the CW and SESAM mode-locked lasers without any extra elements. The approach was simple to implement, and gave a high output polarization ratio for CW operation. Further work on the mode-locked laser involves the optimising SESAM mode-locking system and the introduction of the dispersion compensation elements, to allow the production of shorter pulsewidth with a higher polarization ratio.

This work was supported by the Beijing elitist fund and Ph. D. fund from Beijing University of Technology. M. Song's e-mail address is yrsong@bjut.edu.cn.

References

1. A. Lucca, M. Jacquemet, F. Druon, F. Balembois, P. Georges P. Camy, J. L. Doualan, and R. Moncorgé, Opt. Lett. **29,** 1879 (2004).
2. F. Druon, P. Balembois, P. Georges, A. Brun, A. Courjaud, C. Hönninger, F. Salin, A. Aron, F. Mougel, G. Aka, and D. Vivien, Opt. Lett. **25,** 423 (2000).
3. S. C. Zeller, L. Krainer, G. J. Spühler, K. J. Weingarten, R. Paschotta, and U. Keller, Appl. Phys. B **76,** 787 (2003).
4. M. J. Lederer, M. Hildebrandt, V. Z. Kolev, B. Luther-Davies, B. Taylor, J. Dawes, P. Dekker, J. Piper, H. Tan, and C. Jagadish, Opt. Lett. **27,** 436 (2002).
5. F. Brunner, G. J. Spühler, J. Ausder Au, L. Krainer, F. Morier-Genoud, R. Paschotta, N. Lichtenstein, S. Weiss, C. Harder, A. A. Lagataky, A. Abdolvand, N. V. Kuleshov, and U. Keller, Opt. Lett. **25,** 1119 (2000).
6. F. Druon, S. Chénais, P. Raybaut, F. Balembois, P. Georges, R. Gaumé, G. Aka, B. Viena, S. Mohr, and D. Kopf, Opt. Lett. **27,** 197 (2002).
7. H. Liu, J. Nees, and G. Mourou, Opt. Lett. **26,** 1723 (2001).
8. Y. Xue, Q. Wang, Z. Zhang, L. Chai, Z. Wang, Y. Han, H. Sun, J. Li, J. Wang, Y. Wang, X. Ma, and Y. Song, Chin. Opt. Lett. **2,** 466 (2004).
9. P. A. Burns, J. M. Dawes, P. Dekker, J. A. Piper, J. Li, and J. Wang, Opt. Commun. **207,** 315 (2002).